

Sciences and Engineering Research

AIJSER VOL 5 NO 1 (2022) E-ISSN 2641-0311 P-ISSN 2641-0303

Available online at www.acseusa.org
 Journal homepage: <https://www.acseusa.org/journal/index.php/aijsr>
 Published by American Center of Science and Education, USA

SIMULATING THE DRAG REDUCTION MODEL FOR A VEHICLE BY USING VORTEX GENERATOR



Md. Shawkut Ali Khan ^(a) Md. Shamim Rayhan ^(b) Md. Iftakharul Muhib ^{(c)1}

^(a) Professor & Head, Department of Mechanical Engineering, City University, Dhaka, Bangladesh; E-mail: shawkutali8@gmail.com

^(b) Assistant Professor, Department of Mechanical Engineering, Anwer Khan Modern University, Dhaka, Bangladesh; E-mail: mechanicalenvironment10@gmail.com

^(c) Assistant Professor, General Education Department, Faculty of Science and Engineering, City University, Dhaka, Bangladesh; E-mail: muhibiftakhar@gmail.com

ARTICLE INFO

Article History:

Received: 30th October 2022

Accepted: 26th December 2022

Online Publication: 30th December 2022

Keywords:

Drag Reduction, Simulation, Vortex Generator

JEL Classification Codes:

C61, R41, Q51

ABSTRACT

Petroleum fuel consign has been lessening at a very high proportion. Almost all automobiles depend upon an IC engine driven by petroleum fuels. As much as the number of automobiles is developing in this modern world, it is obligated to reduce fuel expenditure. One of the ways to do this is to diminish the car's drag. Among a manifold process of reducing drag, using Vortex Generators is one. Delta-shaped vortex generators are used at the rear trunk of the range rover, where the flow separates. K-epsilon turbulent model in ANSYS-Fluent 19.2 software is used to imitate the airflows. This work observed the number and spacing between successive vortex generators based on comparing drag coefficient values. The contours of static pressure and velocity magnitude were also observed for each model. When the vortex generators were attached, the pressure coefficients at the rear trunk began to increase, confirming the increment in back pressure. Hence, the increase in back pressure indicates a reduction in the drag coefficient. It has been found that a combination of 7 vortex generators is the optimum solution. The devices work better at a higher velocity than the lower velocity without affecting vehicle stability. The vortex - 4 model's drag coefficient was found to be significantly lower than that of the standard model vehicle, which is 0.42877. The Base Model of Range Rover (2020) is my sense of humor, the highest drag coefficient. So vortex generators are commonly used on automobile vehicles to prevent downstream flow separation and improve their overall performance by reducing drag.

© 2022 by the authors. Licensee ACSE, USA. This article is an open access article distributed under the terms and conditions of the Creative Commons Attribution (CC BY) license (<http://creativecommons.org/licenses/by/4.0/>).

INTRODUCTION

Transportation is a major factor of a country's national growth. As a developing country, the govt. of Bangladesh gives huge attention to transport sector to strengthen the way of development. Peoples 180 million population of Bangladesh use different types of transport system to maintain their livelihood, such as, bus, minibus, microbus, private car, human hauler, Nosimon etc. Automobile industry's improvement initiated in the 17th century with the invention of the first steam power vehicle which was able of human conduction. In the 19th century, the first internal combustion was invented. The productions of vehicles have been started from 1900 to 1920 decades. In the beginning, Engineers were neglected the ground effect and the balance of the airflow on the body (Ali et al., 2013). The main intention of this study was to appear the improvement and design of drag reducing devices for an automobile, Range Rover (2020), by studying the vehicle's aerodynamics. Aerodynamics plays vital role in vehicle design. Enhancement prices of oil and the countries movement towards reducing its dependence on imported oil, it is the reasonable part of engineers to trace and develop ways to increase fuel economy. Using the principles of aerodynamics, it is possible to abate the coefficient of drag (C_d) of a vehicle and contribute to its fuel efficiency. Most of the research on the benefits of VGs has been conducted in the field of aviation. Some research has also proven that VGs can generate modest suitability in drag reduction on vehicles. In addition to having the potential to reduce the coefficient of drag (C_d) on a vehicle, also there are other available to using VGs on an automobile vehicle. Example, it can help abate spoil of the rear window. Also, unlike other drag reduction devices currently in the market such as spoilers, wings and front splitters, VGs have a less prominent presence on vehicles, while still providing drag reduction benefits. In addition, they are relatively easy to install and remove without leaving any permanent marks on the mounting surface, which can potentially affect the resale value of a vehicle (Vedrtnam & Sagar, 2019). Due to global economic and climate change,

¹Corresponding author: ORCID ID: 0000-0002-5143-2482

© 2022 by the authors. Hosting by ACSE. Peer review under responsibility of American Center of Science and Education, USA. <https://doi.org/10.46545/aijsr.v5i1.292>

To cite this article: Khan, M. S. A., Rayhan, M. S., & Muhib, M. I. (2022). SIMULATING THE DRAG REDUCTION MODEL FOR A VEHICLE BY USING VORTEX GENERATOR. *American International Journal of Sciences and Engineering Research*, 5(1), 31-45. <https://doi.org/10.46545/aijsr.v5i1.292>

automotive sectors concentrated on lowering fuel costs by minimizing the drag of their cars. To counteract the negative effects on the national energygrid, reduce your energy consumption. The actions below would be taken to do additional researchand analysis, and the research's findings could be amended in light of Bangladesh.

- To create and configure the vehicle models for the vortex generators experiment, and to measurethe experimental aerodynamic drag parameters.
- ANSYS 19.2 and advanced aerodynamic technology to simulate the vehicle model for theparameters of the vehicle.

Thus, this research's output will investigate alternative VG designs and the ideal angle of attack to determine the best drag-reduction configuration for this generic Range Rover 2020. The efficiencyof VGs at various speeds will also be investigated. The proposed Range Rover 2020 model aerodynamic advantage can suit current local transportation needs, requiring less energy to movedown the road while also providing the following facilities.

- From an economic perspective, it is advantageous for the country's energy usage.
- To improve fuel economy.
- To save the environment worldwide.

LITERATURE REVIEWS

Many literature reviews published in the field of aerodynamic drag of vehicles. The excessive motive of the review papers is comparing among the papers and to investigate the outcomes of the results. The reference results of the published review papers role of the base model and satisfiedthe results. The application of the review papers in industries depends on the accuracy, low cost and optimum design of the model results. The research presented by Lin (2002) is one of the most cited in the applied aerodynamic research aboutVortex Generator. The idea behind the study of Lin et al. is to ensure the minimum required wall ward momentum transfer and avoid counterproductive VG dimension that would increase the drag.

Alam et al. (2010) studied to overcome the aerodynamic resistance almost 80% (out of total power) of vehicle powers is required and the remaining power is used for rolling resistance. The total fuel cost of thesystem depends on the extra drag due to add-ons causes. The preliminary purpose of this thesis was the aerodynamic drag measure experimentally under the range of vehicle speeds 25 m/sec. A large family size passenger car selected manufacture in Australia which air drag reduced almost 25% of the scale. To reduced aerodynamic drag by modification of the external surface of the bodyand obtain a perfect drag coefficient as well as fuel savings. These modifications do not affect thesafety and operation of the passenger bur. In general, these modifications depend on the low cost and technically skilled person. Drag force is the most momentous to study that happen solid objects move in fluid or gas. Largequantity of force is required to overcome and opposes the direction of the vehicles.

The automotivemanufactures concentrated on reducing the fuel consumption with the lower aerodynamic drag of vehicles. Various researches have been carried out throughout the world for the optimum aerodynamic designs with lower drag also other parameters that increase the fuel consumption. The aerodynamic drag of the vehicles is the main contributor to increase the in fuel consumption. This affects not only the world's fuel reserves but also the environment. When a vehicle moves through in the fluid is defined by a dimensionless value called co-efficient of drag (Cd), drag forcespeed of the fluid. The air pressure act on the face of the object, negative pressure act on the backside and friction act along the sides of the bus. There are two types of drag such as pressure drag and friction drag. The pressure drags acting on the body (normal to vehicle surface) tend to compress the frontal area of the body when moving through the fluid. Friction drag occurred between body and fluid particles (tangential to vehicle surface) as well as it can minimize by the smoothness of the body. The main focus is on the aerodynamics drag reduction as well as fuel consumption, CO₂ reduction. So that's a model design with the optimum aerodynamic drag and improved fuel efficiency (Koike et al., 2004). Aerodynamics on ground vehicle the drag forces are directly related with the shape of the vehicle. That forces, the vehicle must overcome the rolling resistance, changing in acceleration, elevation,climbing angle, driveline friction and also aerodynamics. Considering the vehicle moves on a flatroad at constant speed and external forces are limited to the tires (Dubey et al., 2013).

Table 1. Drag coefficient of existing different vehicle body

Vehicle Type	Aerodynamic Resistance Coefficient (CD)
Passenger Cars	0.30 – 0.52
Vans	0.40 – 0.58
Buses	0.50 – 0.8
Tractor-Semitrailers	0.64 – 1.10
Truck-Trailers	0.74 – 1.00

Yadav et al. (2018)

MATERIALS AND METHODS

The model of a vehicle is very major factor considering its safety, comfort and associates operatingcost especially it energy consumption. The total energy consumption of the vehicles, aerodynamicsdrag is most responsible for a major parts of energy consumption which is directly depended on the aerodynamic shape of vehicle. The issue of reducing the ground electric power vehicle's energyconsumption emerged nearly at the same time when vehicle itself was invented (Askar et al., 2018). Due to numerical analysis of aerodynamic drag and performance of existing models of vehicle, themodelling in which the geometries shape of the reference and non-tested configurations are createdin the surface modelling software Space Claim. The scale of existing investigated Range Rover (2020) is 4940mm of length, Width 2047mm and 1820mm of height, 2997mm is the

wheelbase and weight of Range Rover is 2178 kg (Khan et al, 2019).

Tables 2. Dimension of Range Rover (2020 Model)

Length	4940mm
Width	2047mm
Height	1820mm
Wheelbase	2997mm

Numerical Modelling

The numerical modelling is a useful tool of engineering design and analysis which is employed to solve a process of physically complex problem these have major two parts that physical/ empirical modelling and theoretical/ analytical modelling, of which, the most mathematical equation established in theoretical modelling cannot be solved analytically but requiring a numerical solution (Askar et al., 2018). The governing equations for fluid mechanics are the Navier Stokes equations. These equations show the relationship between the velocity of the fluid, its density and pressure. Navier-Stokes equations can be expressed as follow (Askar et al., 2018).

$$\begin{aligned}
 \rho \frac{du}{dt} &= \rho g_x + \frac{\partial r_{xx}}{\partial x} + \frac{\partial r_{yx}}{\partial y} + \frac{\partial r_{zx}}{\partial z} - \frac{\partial P}{\partial x} \\
 \rho \frac{dv}{dt} &= \rho g_y + \frac{\partial \tau_{xy}}{\partial x} + \frac{\partial \tau_{yy}}{\partial y} + \frac{\partial \tau_{zy}}{\partial z} - \frac{\partial p}{\partial y} \\
 \rho \frac{dw}{dt} &= \rho g_z + \frac{\partial \tau_{xz}}{\partial x} + \frac{\partial \tau_{yz}}{\partial y} + \frac{\partial \tau_{zz}}{\partial z} - \frac{\partial p}{\partial z} \\
 \rho \left(\frac{\partial u}{\partial t} + u \frac{\partial u}{\partial x} + v \frac{\partial u}{\partial y} + w \frac{\partial u}{\partial z} \right) &= - \frac{\partial P}{\partial x} + \rho g_x + \mu \left(\frac{\partial^2 u}{\partial x^2} + \frac{\partial^2 u}{\partial y^2} + \frac{\partial^2 u}{\partial z^2} \right) \\
 \rho \left(\frac{\partial v}{\partial t} + u \frac{\partial v}{\partial x} + v \frac{\partial v}{\partial y} + w \frac{\partial v}{\partial z} \right) &= - \frac{\partial P}{\partial y} + \rho g_y + \mu \left(\frac{\partial^2 v}{\partial x^2} + \frac{\partial^2 v}{\partial y^2} + \frac{\partial^2 v}{\partial z^2} \right) \\
 \rho \left(\frac{\partial w}{\partial t} + u \frac{\partial w}{\partial x} + v \frac{\partial w}{\partial y} + w \frac{\partial w}{\partial z} \right) &= - \frac{\partial P}{\partial z} + \rho g_z + \mu \left(\frac{\partial^2 w}{\partial x^2} + \frac{\partial^2 w}{\partial y^2} + \frac{\partial^2 w}{\partial z^2} \right)
 \end{aligned}$$

By the time-average the Navier Stokes Equation (5.2), the Reynolds Average Navier StokesEquations are obtained (Sen et al., 2019) as

$$\rho \bar{u}_j \frac{\partial \bar{u}_i}{\partial x_j} = \rho \bar{f}_i + \frac{\partial}{\partial x_j} [-\bar{P} \delta_{ij} + 2\mu \bar{S}_{ij} - \rho \bar{u}_i \bar{u}_j]$$

The $(k-\varepsilon)$ turbulence model is robust and widely used despite its limitation. It is easy to implement, computationally cheap and especially valid for fully turbulence flow. It is also suitable for initial iterations, initial screening of alternative design and parametric studies.

The $(k-\varepsilon)$ turbulence model runs through the equations are stated as bellow, where 'k' is the turbulent kinetic energy. The turbulent kinetic energy 'k'

$$\frac{\partial}{\partial t} (\rho k) + \frac{\partial}{\partial x_i} (\rho k u_i) = \frac{\partial}{\partial x_j} \left\{ \left(\mu + \frac{\mu_t}{\sigma_k} \right) \frac{\partial k}{\partial x_j} \right\} + P_k + P_b + \rho \varepsilon - Y_M + S_k$$

And, for dissipation 'ε' model

$$\frac{\partial}{\partial t} (\rho \varepsilon) + \frac{\partial}{\partial x_i} (\rho \varepsilon u_i) = \frac{\partial}{\partial x_j} \left\{ \left(\mu + \frac{\mu_t}{\sigma_\varepsilon} \right) \frac{\partial \varepsilon}{\partial x_j} \right\} + C_{1\varepsilon} \frac{\varepsilon}{k} (P_k + C_{3\varepsilon} P_b) - C_{2\varepsilon} \frac{\varepsilon^2}{k} + S_\varepsilon$$

Where the turbulence viscosity (μ_t) is modeled as

$$\mu_t = \rho C_\mu \frac{k^2}{\varepsilon}$$

And, Product of 'k'

$$P_k = -\rho \bar{u}_i \bar{u}_j \frac{\partial u_j}{\partial x_i}$$

$$P_k = \mu_t S^2$$

And model constant:

$$C_{1\epsilon} = 1.44, C_{2\epsilon} = 1.92, C_\mu = 0.09 \quad \sigma_k = 1.0 \text{ and } \sigma_z = 1.3$$

And, the simulation operating relative model Shear Stress Transport (SST) is a variant of the standard $k-\omega$ model. Combining with original the $k-\epsilon$ model for near walls and standard the $k-\epsilon$ model away from walls. Similar to the $k-\epsilon$ model, the $k-\omega$ model is defined two equation model as below (Sen et al., 2019).

The Turbulence Kinetic Energy (k) for $k-\omega$ model can be written as

$$\frac{\partial k}{\partial t} + U_j \frac{\partial k}{\partial x_j} = P_k - \beta * k\omega + \frac{\partial}{\partial x_j} \left\{ (v + \sigma_k v_T) \frac{\partial k}{\partial x_j} \right\}$$

$$\frac{\partial \omega}{\partial t} + U_j \frac{\partial \omega}{\partial x_j} = aS^2 - \beta\omega^2 + \frac{\partial}{\partial x_j} \left\{ (v + \sigma_{\omega 1} v_T) \frac{\partial \omega}{\partial x_j} \right\} + 2(1 - F_1)\sigma_{\omega 2} \frac{1}{\omega} \frac{\partial \omega}{\partial x_i} \frac{\partial \omega}{\partial x_i}$$

And, specific dissipation rate (ω)

$$\alpha = \frac{5}{9}, \beta^* = \frac{9}{100}, \sigma_{\omega 1} = 0.5 \text{ and } \sigma_{\omega 2} = 0.856$$

Where constant,

The analysis of the flow field with CFD solver can be driven through the two models of mathematical solutions are defined as turbulent kinetic energy (TKE) $k-\epsilon$ model and shear-stress turbulence (SST) $k-\omega$ model. The $k-\omega$ turbulence model is suitable in the analysis to demonstrate the turbulence effect on the flow, because of its give a good behavior in adverse pressure gradients and separating flow (Askar et al., 2018).

Boundary Condition

For a given computational domain, boundary conditions can be given that over-specify or under-specify the simulation model. This usually results in non-physical solutions or failure of the solution to converge. To predict viscous flow over investigated model have been setting through the standard two equations turbulent $k-\epsilon$ model with suitable initial guess and under relaxation parameters, flow and energy equations are iterated till the residual errors. After completion of flow simulation, a built in CFD solver in the software for generations of report is activated to obtain performance with the starting boundary conditions are (Franck et al., 2009).

- Uniform flow at inlet and null pressure conditions are applied to the outer boundary
- A condition of symmetry is applied to the pre-designed symmetric surface, and
- Non slip condition at the downstream outflow boundary that is user defined function compile to the flow quantities from the interior grid points.
- Slip at the lateral and upper sides.

The following CFD solver settings are taken under simulation to execute over all model of car.

Table 3. Solver setting details

Description	Condition
CFD Simulation	3D
Solver	Pressure-Based
Space	3D
Formulation	Implicit
Time	Steady
Velocity Formulation	Absolute
Gradient Option	Cell-Based
Porous Formulation	Superficial Velocity
Viscous model and Turbulence model settings	
Viscous Model	
Turbulence Model	$k-\epsilon$ (2 eqn.)
K-epsilon Model	Standard
Near-wall Treatment	Standard Wall Functions
Operating Conditions	Ambient
Total Kinetic Energy Prandtl Number	1
Total Dissipation Rate Prandtl Number	1.3
Boundary	Conditions
Magnitude (Measured, Normal to Boundary)	20 m/s (X-direction)

Velocityinlet	Turbulence Specification Method	Intensity and Viscosity Ratio
	Turbulent Kinetic Energy (m^2/s^2)	1
	Turbulent Dissipation Rate (m^2/s^3)	1
Pressure Outlet	Gauge Pressure Magnitude	0 Pascal
	Gauge Pressure Direction	normal to boundary
	Turbulence Specification Method	Intensity and Viscosity Ratio
	Backflow Turbulence Kinetic Energy (m^2/s^2)	1
	Backflow Turbulence Dissipation Rate (m^2/s^3)	1
Wall Zone	No Slip	
Fluid Properties	Fluid Type	Air
	Density	$\rho = 1.225 \text{ (kg/m}^3\text{)}$
	Kinematic viscosity	$\eta = 1.7894e-05 \text{ (kg/(m-s))}$
Scheme		Couple
Time		Steady
Solver		
Gradient		Least Squares Cell Based
Pressure		Second Order
Momentum		Second Order Upwind
Turbulent Kinetic Energy		Second Order Upwind
Turbulent Dissipation Rate		Second Order Upwind
Iteration		Second Order Upwind for 500 Iteration
Flow Courant Number		200
Explicit Relaxation Factors		
Pressure		0.5
Momentum		0.5
Under Relaxation Factors		
Turbulent Kinetic Energy		0.8
Turbulent Dissipation Rate		0.8
Turbulent Viscosity		1
Monitors		
Residual, Statistic and Force Monitors		Drag and Drag Coefficient

As the above scenario, the virtual simulation to the problems considered in the past, for procedural and size limits, numerically impossible to be evaluated and faced only by experimental approach. Some of these problems are related to the non-linear dynamic transient behavior of full vehicle FEM models passing over the obstacles. The ideal numerical solution of this problem is to perform the quasi-static analysis (equilibrium prior to the dynamic simulation) using an implicit code and use the implicit results as initial condition of the dynamic analysis performed with an explicit code (Duni et al., 2003).

Computational Meshing and Iteration

Most of the fluid flow simulation technologies are used completely different meshing, loading and solving methods compared to structural simulation. A note that grid generation is generally challenging because of the alternating permutation of grid of vehicle body. It involves a basic tetrahedral generation and additional layer of wedge elements for better resolution close to the body surface. It is sequentially done by the line meshing, surface meshing, volume meshing and wedge elements tetrahedral meshing in order to obtain better simulations of boundary layer without excessive refinement in the remaining flow domain that the final meshing has both wedge and tetrahedral elements their special consideration is needed for parallel implementation. To begin, car is modeled as a computational grid the grid shape cross section is partitioned into different blocks, with square blocks applied to the inner area of the grid shape and triangular blocks, which are modeled as mesh, are applied near the frame, as is shown in Figure 1.

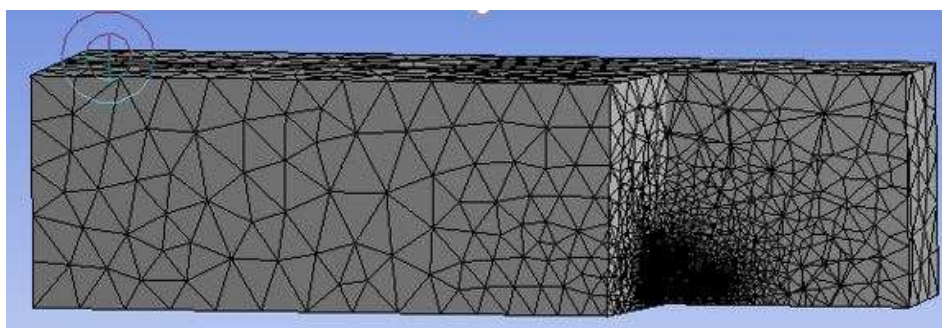


Figure 1. The Mesh of Range Rover (2020)

The geometric models have done using the tetrahedral meshing elements that are easy to fit in small corners and are efficient enough to give accurate results. The meshing grids were divided into coarse, medium and fine meshing grids and the optimum number of meshing elements that have been achieved during the numerical analysis and using the available ANSYS FLUENT software in bellow Table 4.

Table 4. Number of meshing Elements and node during analysis

Models	No of Elements	No of Node
Base Model Car	629345	116691
Vortex -1	634175	117045
Vortex -2	641781	118420
Vortex -3	651994	120250
Vortex -4	660515	121742
Compare Vortex -4	664135	121807
Vortex -5	666154	122780
Vortex -6	672002	122929
Vortex -7	672002	123967

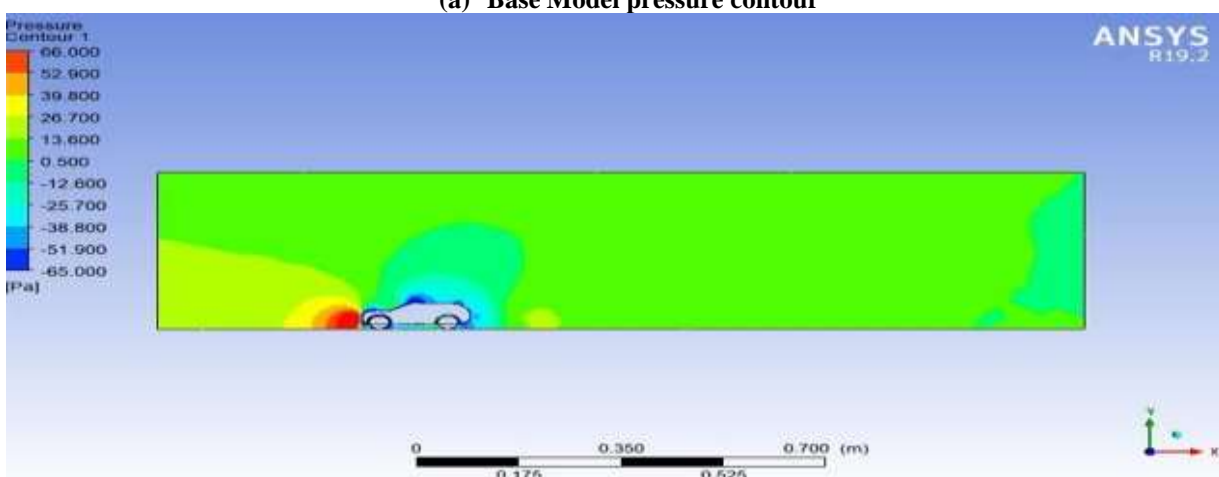
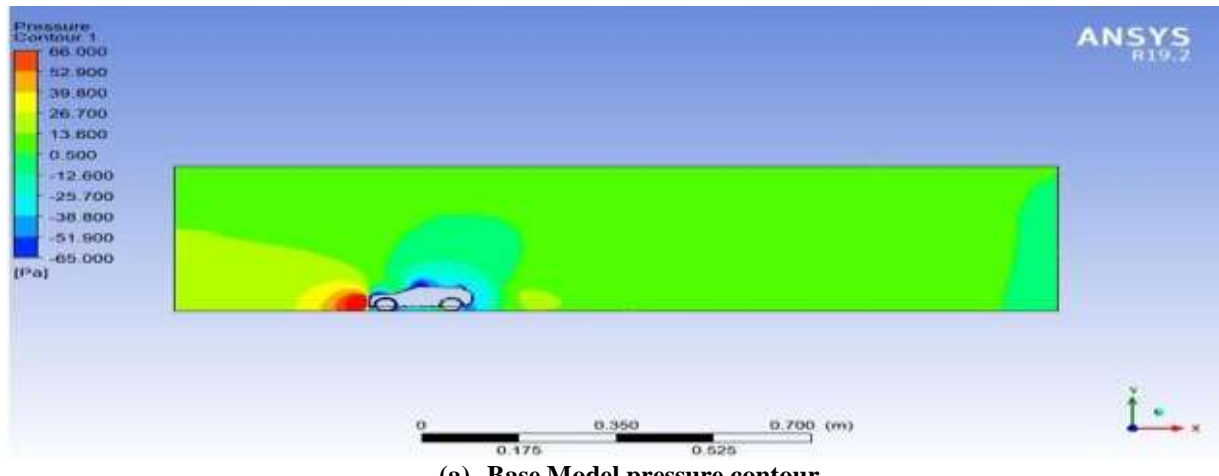
The mesh used for the investigated model was comprised of 6174416 tetrahedral elements. The tetrahedral elements were best used while in the last step a higher order turbulence model is used in conjunction with the fine mesh settings (Lanfrat, 2005). The comparison of the convergent values of drag coefficient (CD) and drag force (FD) obtained from the results of the CFD simulations performed over the all model.

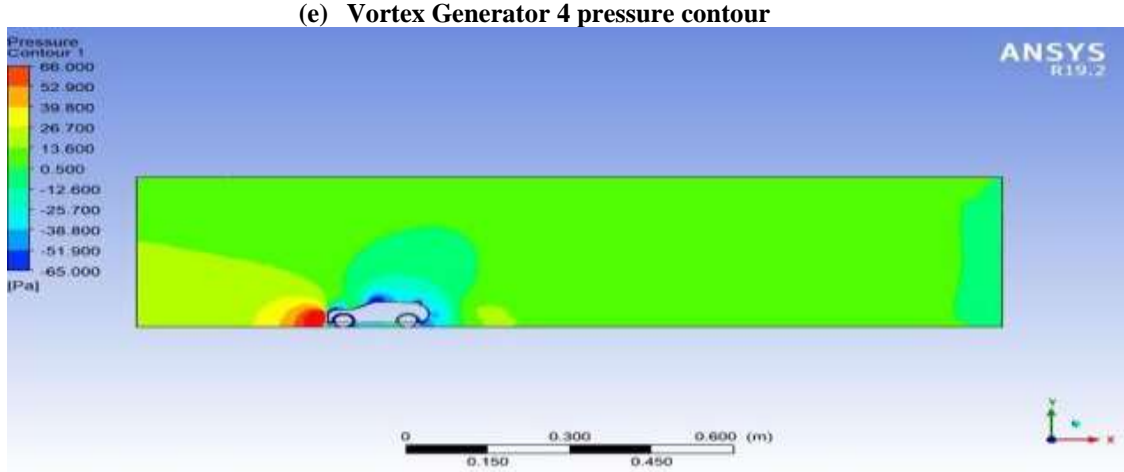
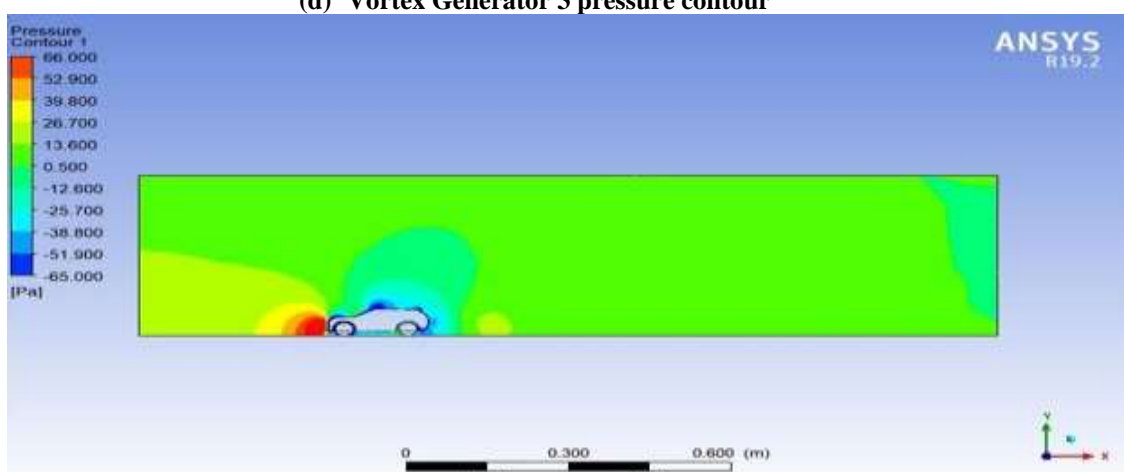
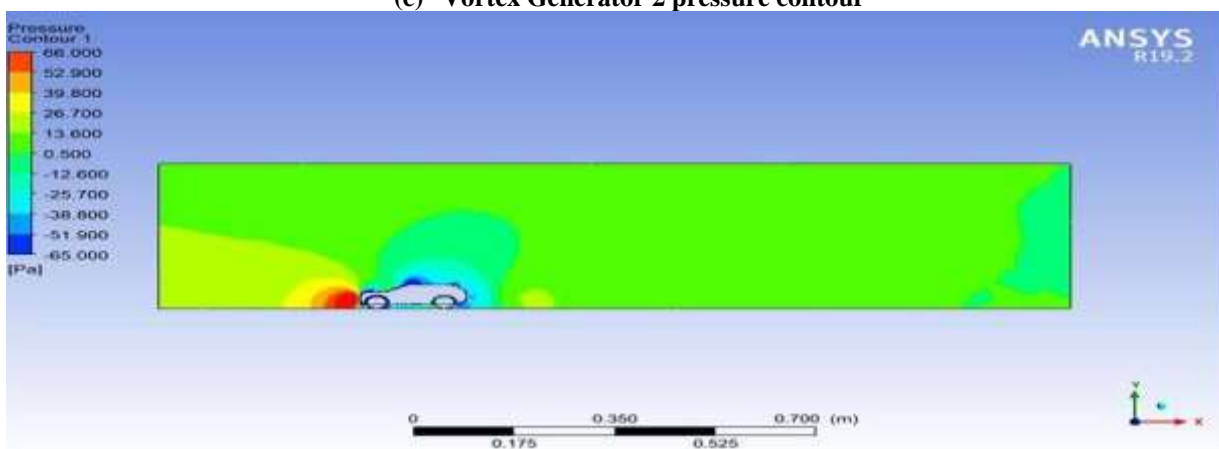
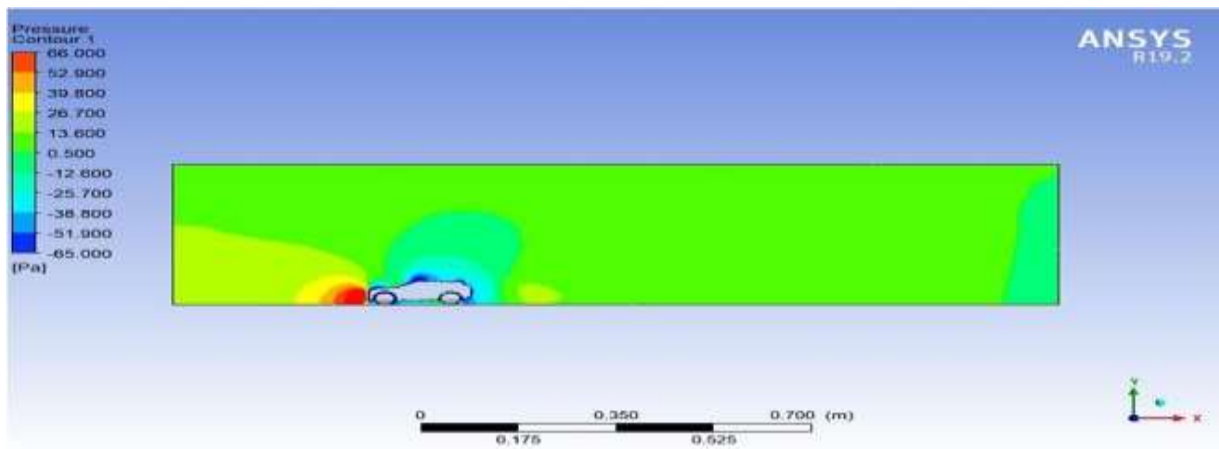
RESULTS AND DISCUSSIONS

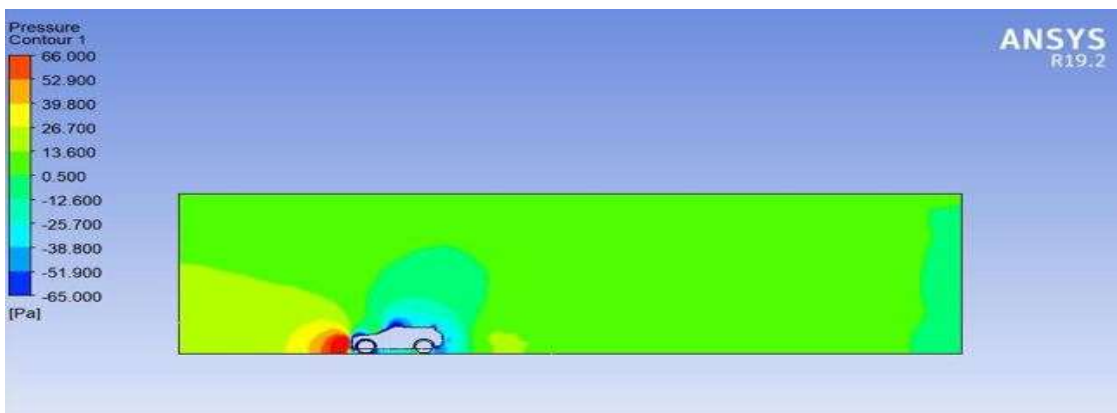
Total seven models of Range Rover (2020) have been investigated numerically. Using the simulation result, the pressure difference and force acting in the direction of flow (i.e. the thrust acting against the direction of propulsion) is calculated. The analyzed simulation results are showing in the following sub sections respectively.

Pressure Contour

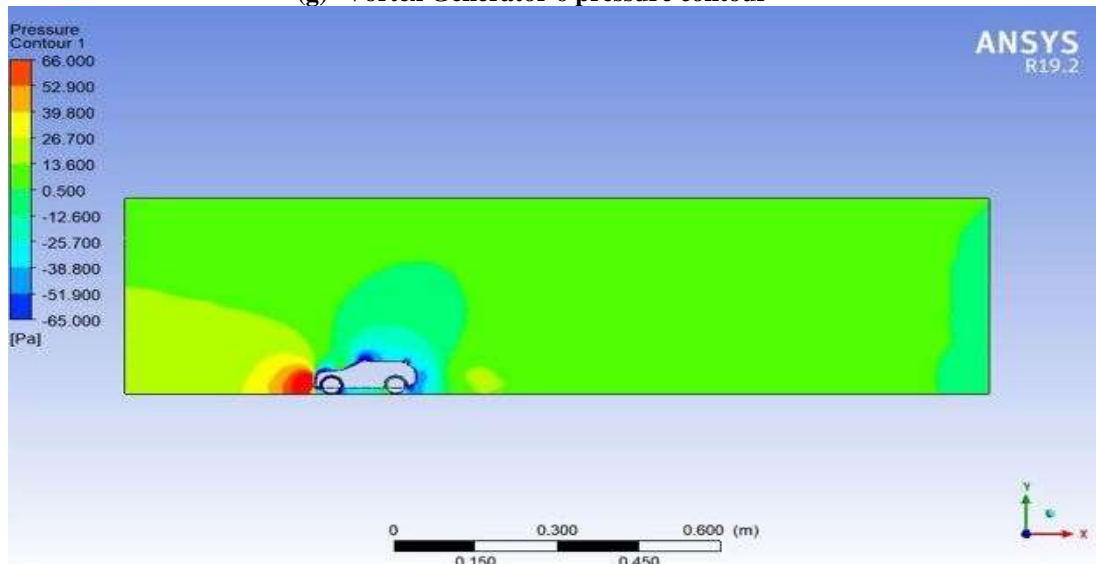
Pressure contour represent the air impacts on vehicle, which helps to investigate the drag contribution. Fig. 2 (a-i) shows that the pressure contours for seven models. In figure 2 (h) to 2 (i) with six and seven numbers of VG and aerodynamic friendly model have 10% reduction in pressure due to modification over the exiting model of base Range Rover 2020.







(g) Vortex Generator 6 pressure contour

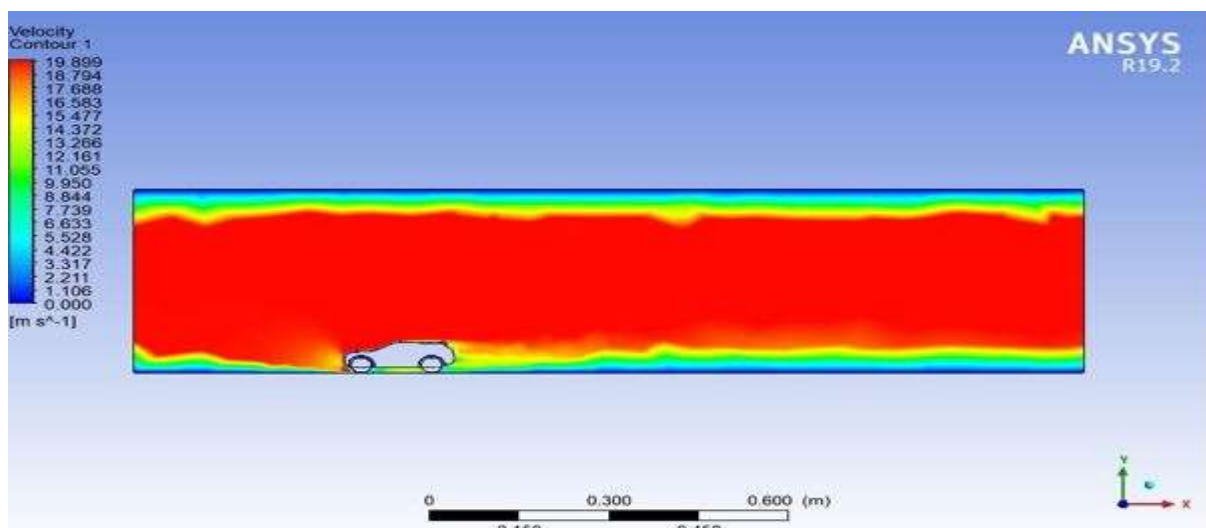


(h) Vortex Generator 7 pressure contour

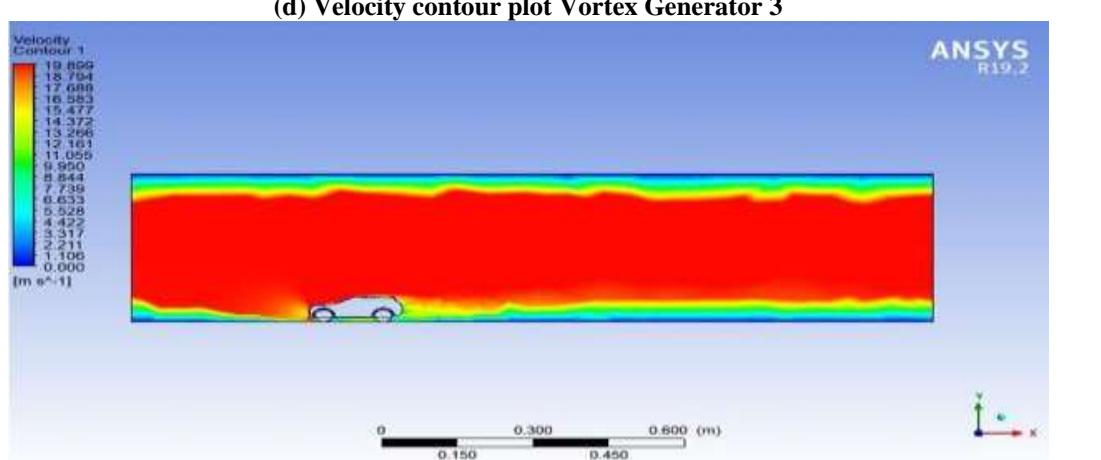
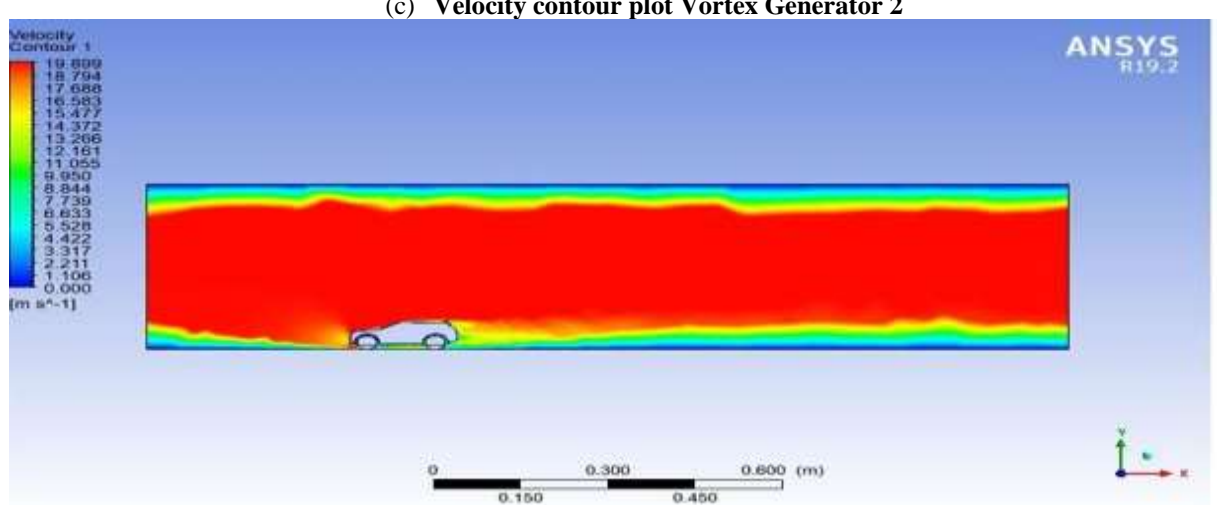
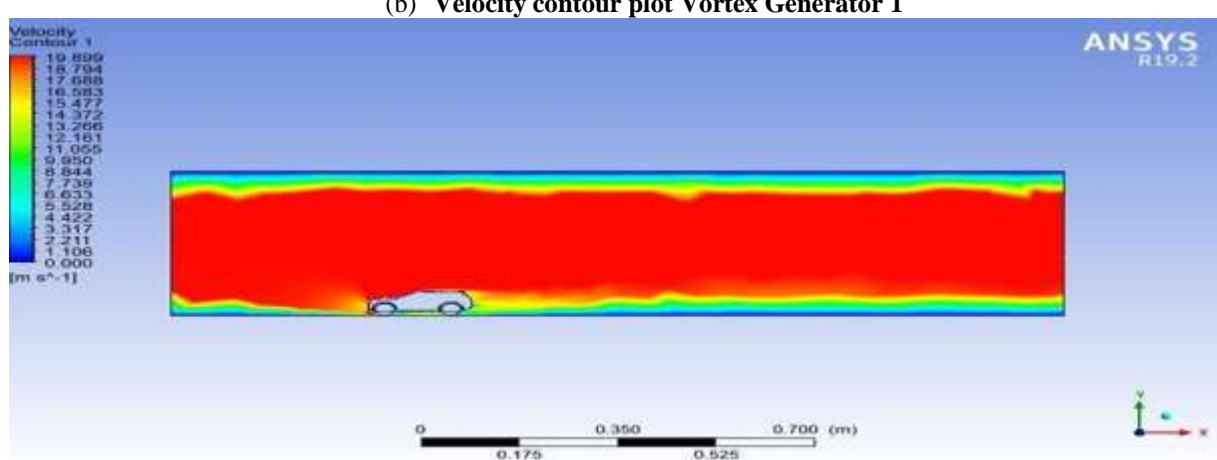
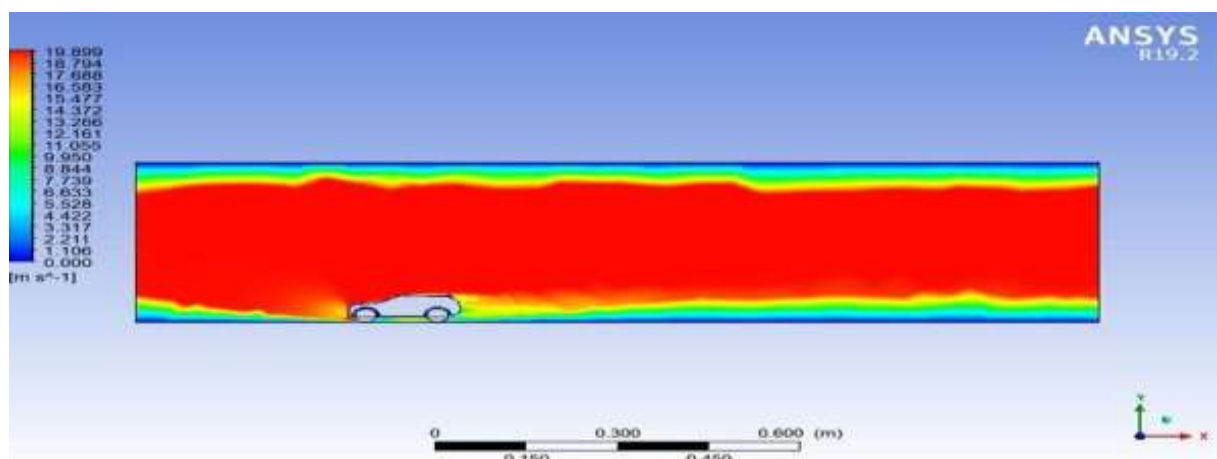
Figure 2. (a-h): Pressure Contour of Range Rover

Velocity Contour Plot

Details of flow around the models are represented by velocity contour which is shown in Fig. 3 (a-i). There are remarkable differences have been found between base models & modification models.



(a) Velocity contour plot Base model



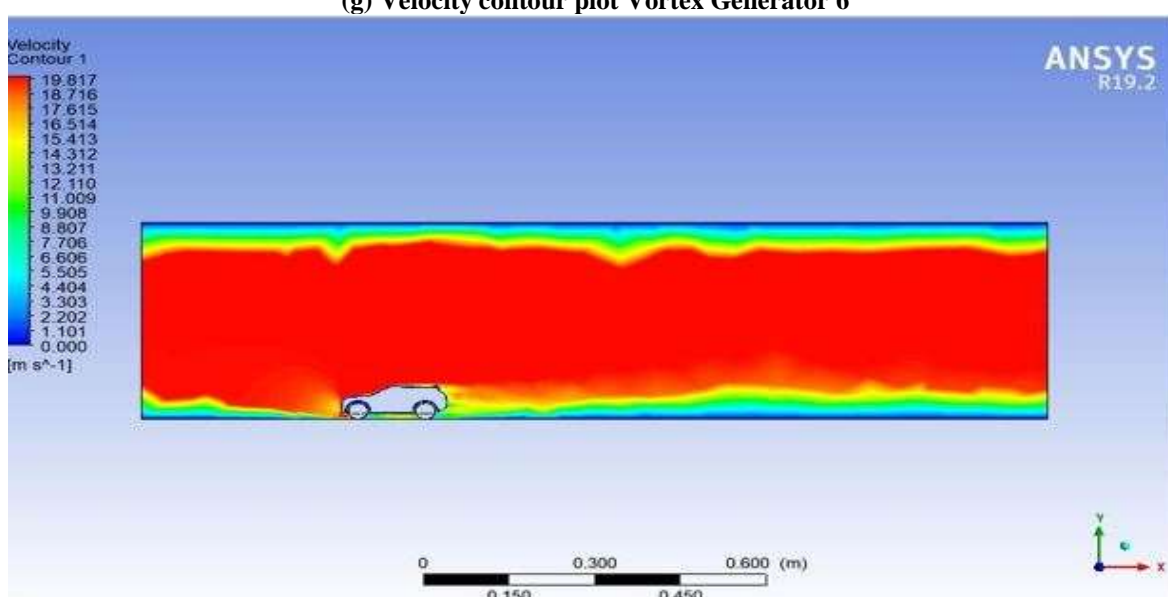
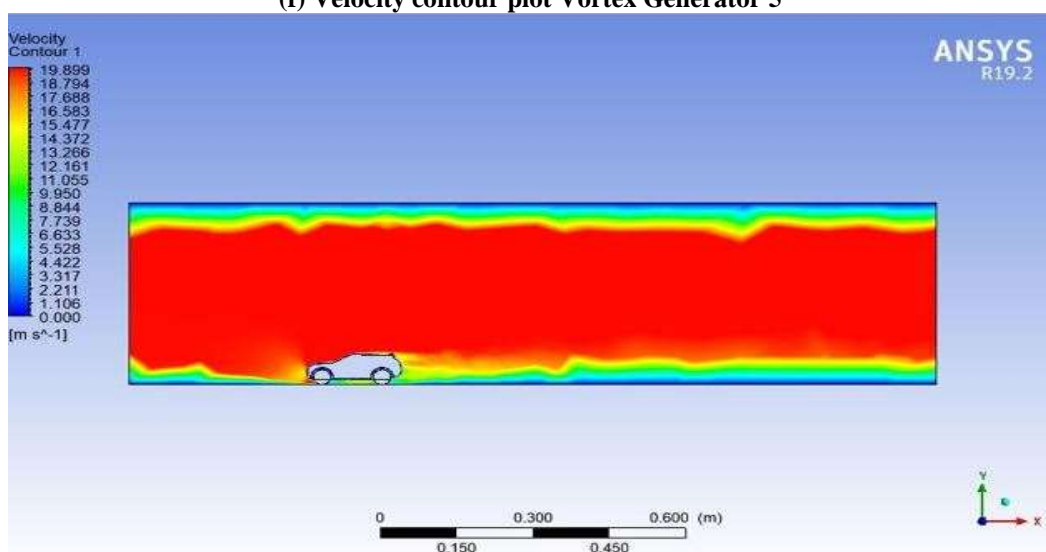
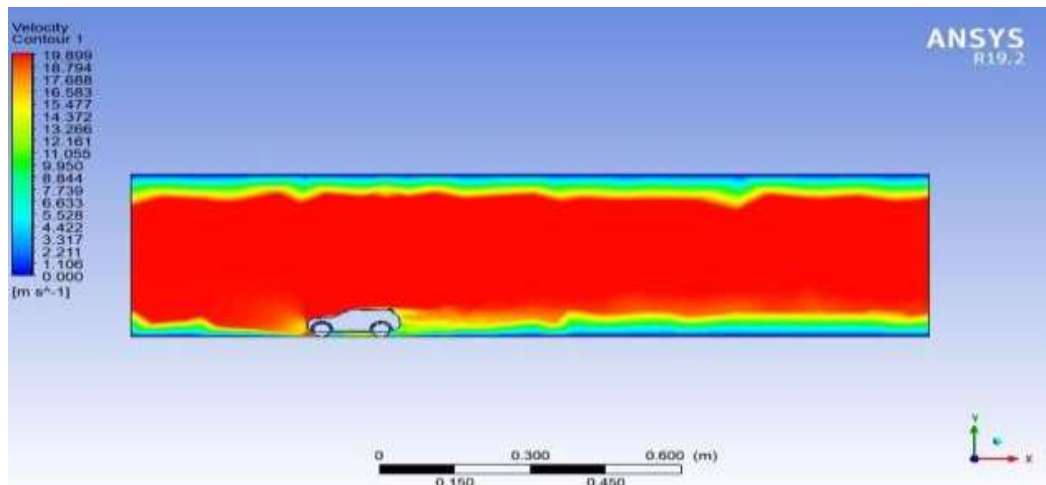
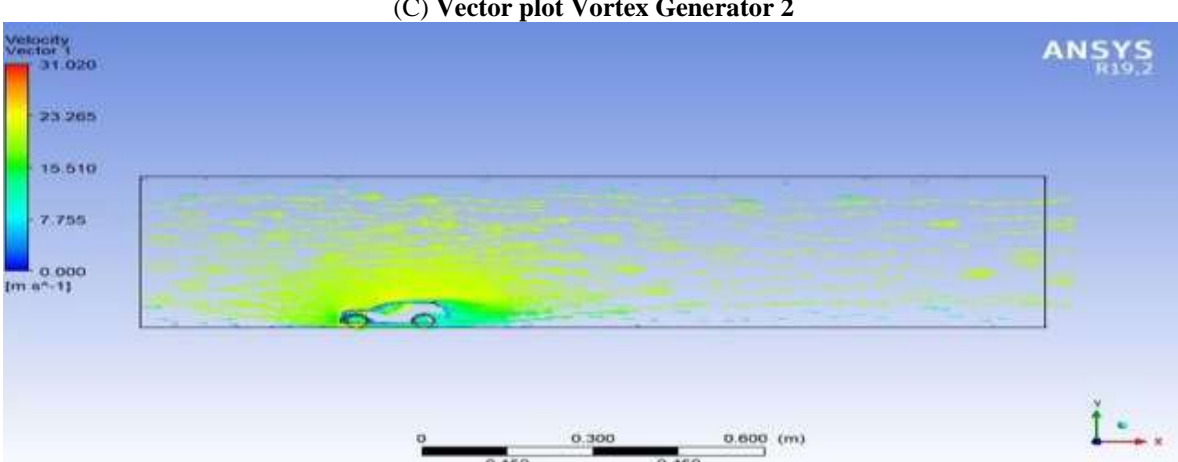
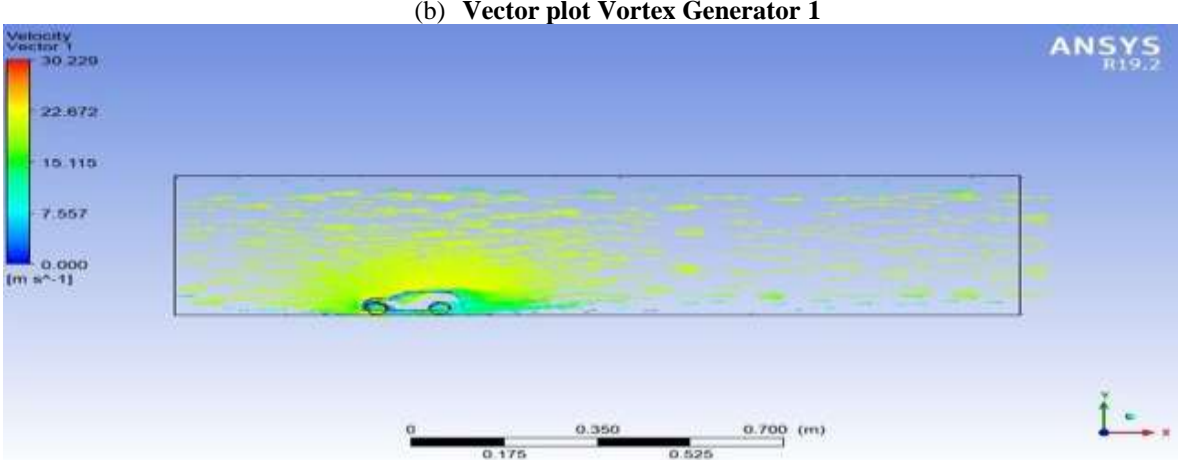
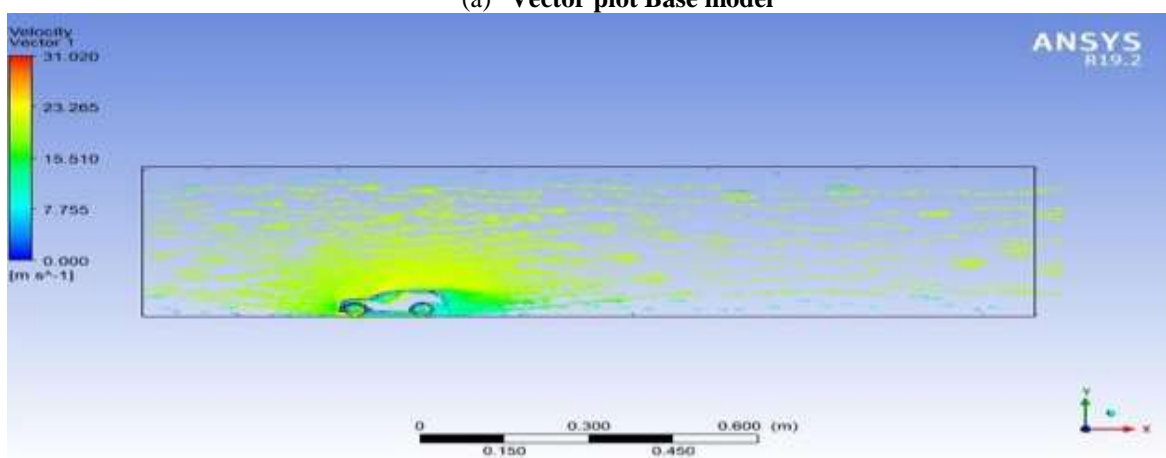
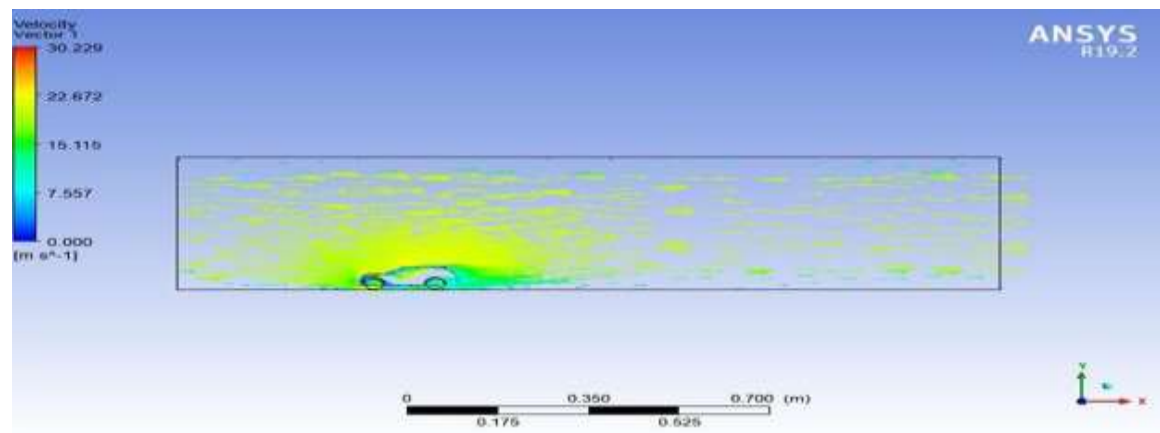


Figure 3. (a-h): Velocity contour plot

Vector Plot

In Figure 4 (a-h), Near wall velocity vector are shown. These vector plots significantly show that these separated flow over the top.



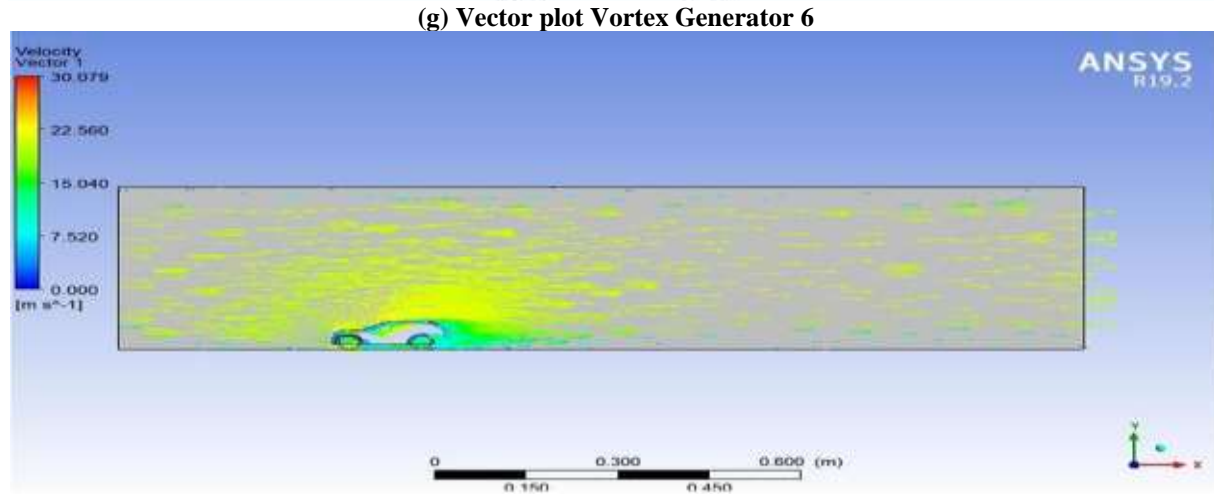
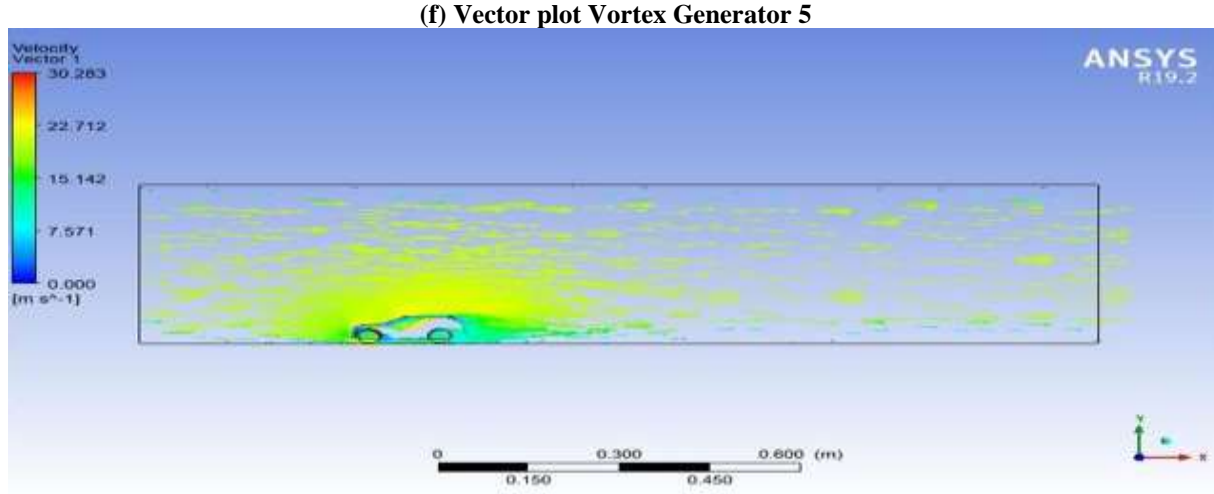
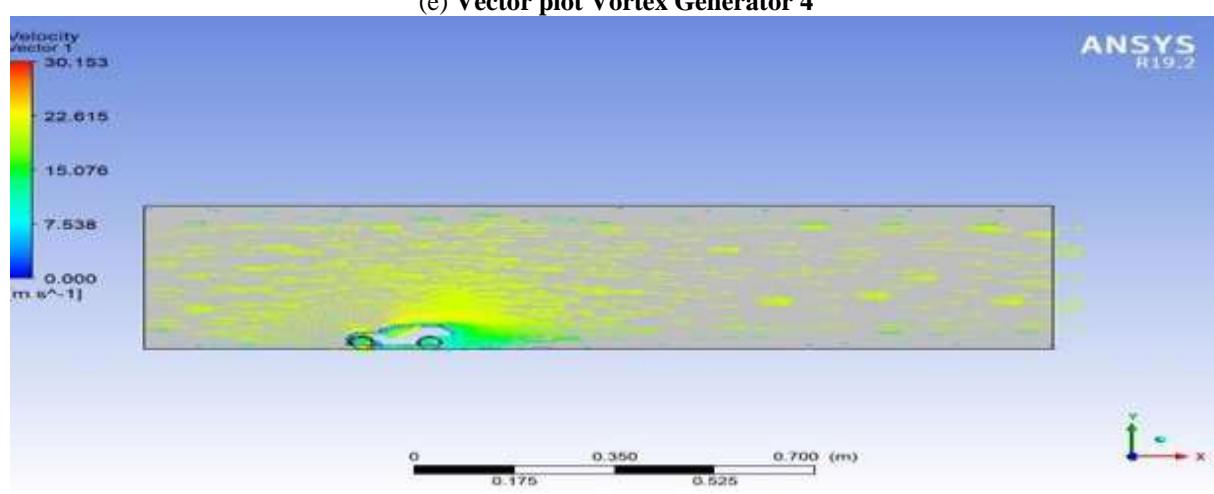
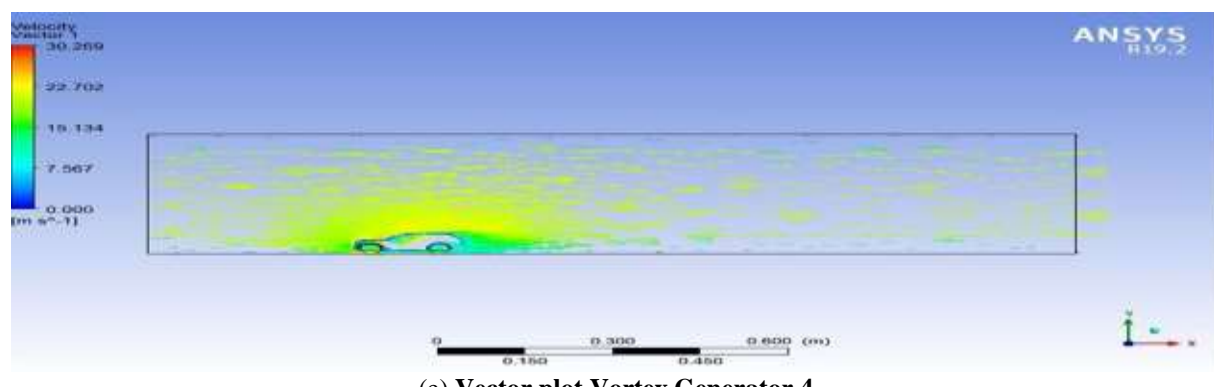


Figure 4. (a-h): Vector plot for Range of Rover

Drag Calculation

To research the effects of car exterior body forms, which produce drag force and coefficient of drag when it is pushed along a road and all of these data are numerically determined. Two existing models with the same size are simulated and their drag force (FD) and coefficient of drag are numerically calculated (CD).

The basic formula for overall drag is given by:

$$D = \frac{\rho}{2} C_d A V^2$$

Where,

C_d =Coefficient of Drag

A=Frontal Area

V=Relative velocity of the object fluid medium

ρ =Density of Air

The same method has also been used to determine the best drag coefficient form for the energy economic model. The Space Claim software was used to create the virtual body shapes for car, and all perimeters were taken into consideration while developing generic models for numerical analysis. The front face experiences a significant impact during the computation of the FD and CD values on the car models that are currently in use, which is a substantial contributor to the creation of the maximum drag. Additionally, it mentions that the front face under shape, front face under form, back side upper shape, and under body arrangement are the points at fault. Numerous large models that had essentially developed in terms of front face and back side modification have been the subject of a numerically labor-saving analysis.

Table 5. Values of drag coefficient of test models in simulation

Experimental Model (s)	Effect of drag and drag co-efficient for both models	
	Drag force, (FD)	Drag coefficient (CD)
Base Model Car	3.5124	2.5295
Vortex -1	0.9384	0.66846
Vortex -2	0.6104	0.43480
Vortex -3	0.6080	0.43316
Vortex -4	0.6019	0.42877
Compare Vortex -4	0.6059	0.42977
Vortex -5	0.6065	0.43208
Vortex -6	0.6109	0.43520
Vortex -7	0.6161	0.43890

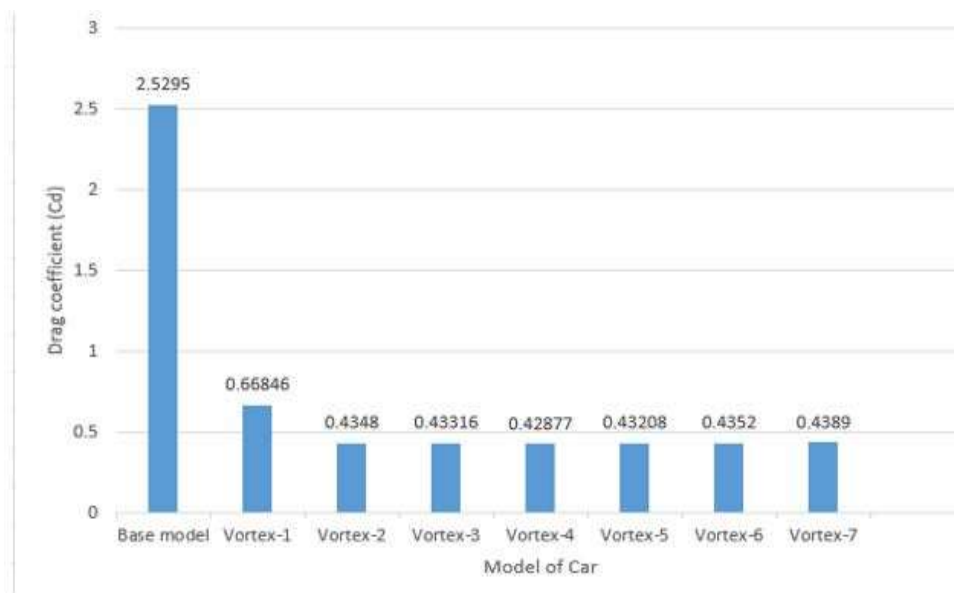


Figure 5: Drag coefficient (Cd) of investigated eight models of Car

It is discovered that the vortex -4 model's drag coefficient is significantly lower than that of the standard model car. It is now evident that the only way to significantly lower drag force is to change the design of the body's drag coefficient.



Figure 6. Plot of the Drag Coefficient (C_d) of eight model of Car

This figure shows that the X, Y graph between drag coefficient and model of car with several vortex generators. Drag coefficient are in Y axis and base model with seven vortex generators are in X axis. From the X, Y graph its shown that the base models drag coefficient is 2.5295, when the one vortex generator add on the vehicle the drag coefficient decrease at 0.66486 point. From the two vortex generators to seven vortex generators added it is quite same as we can see in the figure. Though the four vortex generators drag coefficient (0.42877) is lower than other vortex generators.

CONCLUSIONS

The installation of vortex generators causes the boundary layer to gain energy, which improves the adhesion of the airflow to the vehicle's body surface from the roof to the rear part. Without a vortex generator, the flow is clearly split towards the back of the car, according to simulation figures. An analysis has been done to investigate the effect of advanced aerodynamic designs for drag reduction Range Rover 2020 model vehicle. A Computational Fluid Dynamic (CFD) analysis has been done using ANSYS R19.0 workbench. Base model of Range Rover 2020 and seven vortex generators with sequencing run on this thesis. Some modification of the body such as rear side area which affects the aerodynamics on the vehicle. Firstly, demo model or base model analysis by simulation with the experimental result seen and the Base model coefficient of drag is 2.5295 which is very high instead of four vortex generator on Range Rover 2020 which is 0.42877 very low than others.

It is revealed that drag can be reduced by modifying the outer shape. Among all the model investigated numerically the last modification of seven vortex generator with Range Rover 2020 model provides lowest drag coefficient (C_d) which is 0.42877 compare with the model base model which highest value of drag is 2.5295. It is evident from the results and simulation comparisons that adding vortex generators decreases drag and increases downward force while decreasing boundary layer separation. The conclusion may, therefore, eventually be drawn that vortex generators were created with the intention of increasing fuel efficiency and enhancing vehicle aerodynamic stability by reducing drag. It has been seen that the aerodynamic drag on a vehicle directly affects not only is fuel consumption but also the generation of carbon dioxide (CO_2) from the combusted fuel which directly affected on the environment. In this experiment coefficient of drag is reduced 2.1 by using vortex generators.

To conduct simulation-based tests to investigate various approaches and evaluate them against other prototype model factors, such as altering the vehicle configuration and angle, in order to find the best option that minimizes aerodynamic drag. The effectiveness investigation is required to experimental data, simulation test to ensure the results, validity of the models and to find out the optimal aerodynamic drag.

To investigate the positive and negative effects that combining different technologies with the fundamental body of the models will have on the Range Rover 2020. To gain the models of Range Rover 2020 3D printed by Solid works, after doing this you should done wind tunnel test with experimental and numerical analysis and optimum the results those are important for Bangladesh automobiles sectors. Regarding the responsible another factors of energy consumption might be considered surface finishing, Range Rover (2020) vehicles performance and controlling systems can be analyzed and updated to improve its overall performance.

Author Contributions: Conceptualization, M.S.A.K., M.I.M., and M.S.R.; Methodology, M.S.A.K.; Software, M.S.A.K.; Validation, M.S.A.K.; Formal Analysis, M.S.A.K.; Investigation, M.S.A.K.; Resources, M.S.A.K., M.I.M., and M.N.; Data Curation, M.I.M.; Writing – Original Draft Preparation, M.I.M.; Writing – Review & Editing, M.S.A.K., M.I.M., and M.S.R.; Visualization, M.S.A.K., M.I.M., and M.S.R.; Supervision, M.S.A.K.; Project Administration, M.S.A.K.; Funding Acquisition, M.S.A.K., M.I.M., and M.S.R. Authors have read and agreed to the published version of the manuscript.

Institutional Review Board Statement: Ethical review and approval were waived for this study, due to that the research does not deal with vulnerable groups or sensitive issues.

Funding: The authors received no direct funding for this research.

Acknowledgement: Not applicable.

Informed Consent Statement: Informed consent was obtained from all subjects involved in the study.

Data Availability Statement: The data presented in this study are available on request from the corresponding author. The data are not publicly available due to restrictions.

Conflicts of Interest: The authors declare no conflict of interest.

REFERENCES

Alam, F., Chowdhury, H., Moria, H., & Watkins, S. (2010). Effects of vehicle add-ons on aerodynamic performance. In *The Proceeding of the 13th Asian Congress of Fluid Mechanics (ACFM2010)* (p. 186).

Ali, M. H., Mashud, M., Al Bari, A., & Islam, M. M. U. (2013). Aerodynamic drag reduction of a car by vortex generation. *International Journal of Mechanical Engineering*, 2(1), 12-21.

Askar, M. K. A., Hameed, A. Q., Suffer, K. H., & Razlan, Z. M. (2018). Numerical simulation of a new spoiler on upper surface of Clark Y14 wing. In *IOP Conference Series: Materials Science and Engineering* (Vol. 429, No. 1, p. 012080). IOP Publishing. Retrieved from <https://iopscience.iop.org/article/10.1088/1757-899X/429/1/012080/meta>

Dubey, A., Chheniya, S., & Jadhav, A. (2013). Effect of Vortex generators on Aerodynamics of a Car: CFD Analysis. *International Journal of Innovations in Engineering and Technology (IJIET)*, 2(1), 137-144. Retrieved from <https://citeseerx.ist.psu.edu/document?repid=rep1&type=pdf&doi=b9a90aa72877b519d5232f25383a5b28bc344173>

Duni, E., Monfrino, G., Saponaro, R., Caudano, M., Urbinati, F., Marco, S., & Antonino, P. (2003). Numerical simulation of full vehicle dynamic behaviour based on the interaction between ABAQUS/Standard and explicit codes. In *Abaqus Users' Conference, june Munich*.

Franck, G., Nigro, N., Storti, M., & D'elia, J. (2009). Numerical simulation of the flow around the Ahmed vehicle model. *Latin American applied research*, 39(4), 295-306. Retrieved from http://www.scielo.org.ar/scielo.php?pid=S0327-07932009000400003&script=sci_arttext&tlng=en

Khan, F. N., Batul, B., & Aizaz, A. (2019, October). A CFD analysis of wingtip devices to improve lift and drag characteristics of aircraft wing. In *IOP Conference Series: Materials Science and Engineering* (Vol. 642, No. 1, p. 012006). IOP Publishing. Retrieved from <https://iopscience.iop.org/article/10.1088/1757-899X/642/1/012006/meta>

Koike, M., Nagayoshi, T., & Hamamoto, N. (2004). Research on aerodynamic drag reduction by vortex generators. *Mitsubishi motors technical review*, 16, 11-16. Retrieved from Mitsubishi motors technical review, 2004 - s2ki.com

Lanfrit, M. (2005). Best practice guidelines for handling Automotive External Aerodynamics with FLUENT. Retrieved from https://www.southampton.ac.uk/~nwb/lectures/GoodPracticeCFD/Articles/Ext_Aero_Best_Practice_Ver1_2.pdf

Lin, J. C. (2002). Review of research on low-profile vortex generators to control boundary-layer separation. *Progress in Aerospace Sciences*, 38(4-5), 389-420. [https://doi.org/10.1016/S0376-0421\(02\)00010-6](https://doi.org/10.1016/S0376-0421(02)00010-6)

Range Rover (2020). Meet The 2020 Land Rover Range Rover At Land Rover Ocala. Retrieved from <https://www.landroverocala.com/new-range-rover-for-sale-ocala-fl/#:~:text=The%20Standard%20Wheelbase%202020%20Range,with%208%2Dspeed%20automatic%20transmission.>

Sen, W., Rahman, K. A., & Tanim, I. K. (2019). Experimental and CFD analysis on car with several types of vortex generators. In *Proceedings of the international conference on mechanical engineering and renewable energy* (pp. 11-13).

Vedrtnam, A., & Sagar, D. (2019). Experimental and simulation studies on aerodynamic drag reduction over a passenger car. *International Journal of Fluid Mechanics Research*, 46(1). Retrieved from <https://www.dl.begellhouse.com/journals/71cb29ca5b40f8f8,075354f82a6f0e6f,232808716449c7e1.html>

Yadav, A., Rawal, P., & Mishra, R. K. (2018). Modelling and simulation of aerodynamic performance of Vortex generators for hatch back type cars. *Vibroengineering Procedia*, 21, 131-136. Retrieved from <https://www.extrica.com/article/20399>

Publisher's Note: ACSE stays neutral with regard to jurisdictional claims in published maps and institutional affiliations.



© 2022 by the authors. Licensee ACSE, USA. This article is an open access article distributed under the terms and conditions of the Creative Commons Attribution (CC BY) license (<http://creativecommons.org/licenses/by/4.0/>).

American International Journal of Sciences and Engineering Research (E-ISSN 2641-0311 P-ISSN 2641-0303) by ACSE is licensed under a Creative Commons Attribution 4.0 International License.